Organic & Biomolecular Chemistry

COMMUNICATION

View Article Online
View Journal | View Issue

Cite this: *Org. Biomol. Chem.*, 2019, **17**, 1767

Received 21st September 2018,
Accepted 14th November 2018

DOI: 10.1039/c8ob02346h

rsc.li/obc

Mechanism of nitrones and allenoates cascade reactions for the synthesis of dihydro[1,2-*a*] indoles†

Wes Lee,‡ Mingbin Yuan,‡ Christopher Acha,‡ Ashley Onwu and Osvaldo Gutierrez *

Quantum mechanical calculations (DLPNO-CCSD(T) and dispersion-corrected DFT) are employed to gain insights into the mechanism and selectivity in the catalytic synthesis of dihydropyrido[1,2-*a*]indoles from the cascade reaction between nitrones and allenes. Implications for controlling diverging pathways is discussed.

Development of controlled cascade reactions offers the potential to rapidly access diverse chemical library scaffolds for applications in medicinal chemistry and biology.[1] In particular, given the presence of heterocycles in many of the top-selling pharmaceutical drugs,[2] the synthesis of heterocyclic libraries remains a highly active area of chemical research.[3] Tufariello,[4] Uccella,[5] Blechert,[6] Padwa,[7] Ishar,[8] and Anderson[9] have demonstrated the use of *N*-substituted nitrones and allenes precursors towards the synthesis of heterocyclic scaffolds.[10] More recently, Anderson extended the use of cascade reactions between nitrones and allenes towards the diastereoselective catalytic synthesis of dihydropyrido[1,2-*a*] indoles using hydrogen-bonding catalysts (Scheme 1).[11,12] However, the overall mechanism and origin of selectivity for the thermal and thiourea-catalysed reaction and related transformations are poorly understood thus diminishing widespread applicability. Herein we use quantum mechanical calculations (DLPNO-CCSD(T) and dispersion corrected DFT) to gain insights into the mechanism of these cascade reactions. Implications for rational design of cascade reactions using nitrones and allenes as precursors is described.

The working hypothesis for the title cascade reaction is shown in Scheme 2. Addition of nitrone **1** to the electrophilic carbon of the allene **2** leads to the formation of zwitterionic intermediate **A**. In turn, intermediate **A** can undergo a [3,3]-sigmatropic rearrangement/H-shift leading to the formation of enamino-ketone **B**. Facile tautomerization of **B** will then form the corresponding enanimo-enol **C**. From **C**, two divergent pathways are proposed leading to the observed hetereocyclic products **3** and **4**: (1) Intramolecular Mannich addition leading to benzazepine **4** (blue) and (2) Intramolecular hetero Diels–Alder reaction leading to fused indoline **D** (red), which can then undergo dehydration to form dihydropyridoindole **3**. Notably, control experiments determined that the formation of benzazepine **4** is irreversible and does not convert to product **3**. However, the factors controlling the divergent reactivity, selectivity, and mechanism are not known.[8] Herein, we dis-

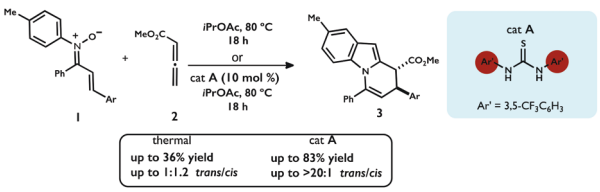

Scheme 1 Synthesis of dihydropyrido[1,2-*a*]indoles *via* cascade reaction from nitrones and allenes reported by Anderson.

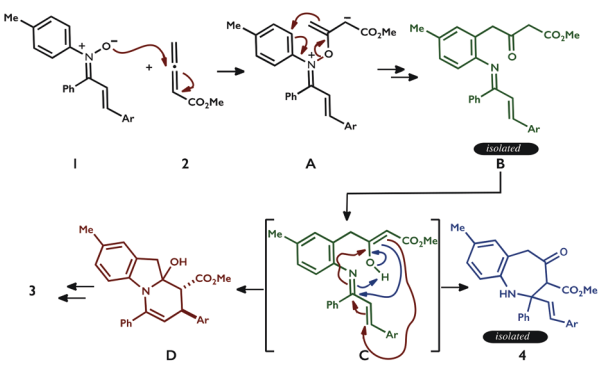

Scheme 2 Proposed mechanisms for the formation of **3** and **4** from nitrone **A** and allenoate **B**.

Department of Chemistry and Biochemistry, University of Maryland, College Park, Maryland 20742, USA. E-mail: ogs@umd.edu

†Electronic supplementary information (ESI) available. See DOI: 10.1039/c8ob02346h

‡These authors contributed equally.

close a detailed quantum mechanical study on these transformations. As representative system, we model all aryl groups as phenyl groups in the nitrone component and no other truncations were applied to the experimental system. Unless otherwise stated, all optimizations were performed at the M06-2X[13]/6-31G(d,p) level of theory in an implicit solvent (chloroform) using CPCM solvation model[14] as implemented in GAUSSIAN09.[15] Further, to refine energetics, we also performed single point energy calculations using Domain-based Local Pair-Natural Orbital Coupled-Cluster singles and doubles method plus perturbative triples (DLPNO-CCSD(T)) using def2-TZVPP basis as implemented in ORCA.[16] The DLPNO-CCSD(T) method is known to provide accurate energies (within 3 kJ mol^{-1})[17] and has recently been applied to study organic reaction mechanisms[18] and non-covalent interactions.[19] Further, for comparison we also performed single point energy calculations using a higher dielectric implicit solvent (water) at the M06-2X/6-31G(d,p)-CPCM level of theory. All 3D structures were generated using CYLview.[20]

We began our mechanistic studies by computing the barrier for the *O*-nucleophilic attack of nitrone **1′** to the most electrophilic internal carbon of the allene **2** (Fig. 1, red). As shown in Fig. 1, the barrier for C–O bond formation is 21–27 kcal mol^{-1} (depending on the method), which are both feasible at experimental conditions, but that will lead to the formation of highly endergonic (14–23 kcal mol^{-1} higher in energy) zwitterionic intermediate **A′**. Given that this intermediate is significantly uphill in energy (even in highly polar solvent) it is unlikely that it can be detected in solution. Nonetheless, from the zwitterionic intermediate **A′**, a subsequent [3,3]-sigmatropic and H-shift cascade reaction could lead to enamino-ketone **B″** (Fig. 1, red). However, the 32–35 kcal mol^{-1} barrier required for the [3,3]-sigmatropic shift (*via* $\mathbf{TS_{[3,3]}}$-**A′**) leading to the corresponding azallenium **B′** intermediate is insurmountable at the experimental conditions! This insurmountable energy barrier led use to considered exploring alternative pathways that would lead to experimentally observed products **3** and **4** without proceeding *via* zwitterionic intermediate **A.**

Previously, a [3 + 2] dipolar cycloaddition between nitrones and allenes followed by [3,3]-sigmatropic shift, and retro-Mannich cascade reaction has been proposed as an alternative pathway leading to the formation of enamino-ketones such as **B″**.[10] As shown in Fig. 1 (green-blue), calculations show that the [3 + 2] dipolar cycloaddition between nitrone **1′** and allene **2** is feasible (overall barrier is only 16–21 kcal mol^{-1}) *via* $\mathbf{TS_{[3+2]}}$ and irreversible (downhill in energy by *ca.* 20–27 kcal mol^{-1}) leading to cycloaddition adduct **A″**. A closer look at the chemo- and regioselectivity of the purported [3 + 2] dipolar cycloaddition is shown in Scheme 3. Calculations demonstrate a significant energetic preference for cycloaddition *via* $\mathbf{TS_{[3+2]}}$-**A-*anti*** (simply labelled as $\mathbf{TS_{[3+2]}}$ in Fig. 1) and $\mathbf{TS_{[3+2]}}$-**A-*syn*** (overall barrier is only *ca.* 16–17 kcal mol^{-1}) forming the diastereomeric *anti* and *syn* **A″**, respectively, adducts exclusively (*i.e.*, **A″**; Fig. 1). Moreover, in all other modes of cycloaddition including modes leading to *exo* methylene (CH_2) regio-isomers ($\mathbf{TS_{[3+2]}}$-**A′-*anti*** and $\mathbf{TS_{[3+2]}}$-**A′-*syn***) or *exo* 2-methoxy-2-oxoethylidene ($CHCO_2Me$) isomers ($\mathbf{TS_{[3+2]}}$-**B-*anti***, $\mathbf{TS_{[3+2]}}$-**B-*syn***, $\mathbf{TS_{[3+2]}}$-**B′-*anti***, and $\mathbf{TS_{[3+2]}}$-**B′-*syn***) are significantly higher in energy (*ca.* 7–15 kcal mol^{-1}) and therefore not productive. A closer

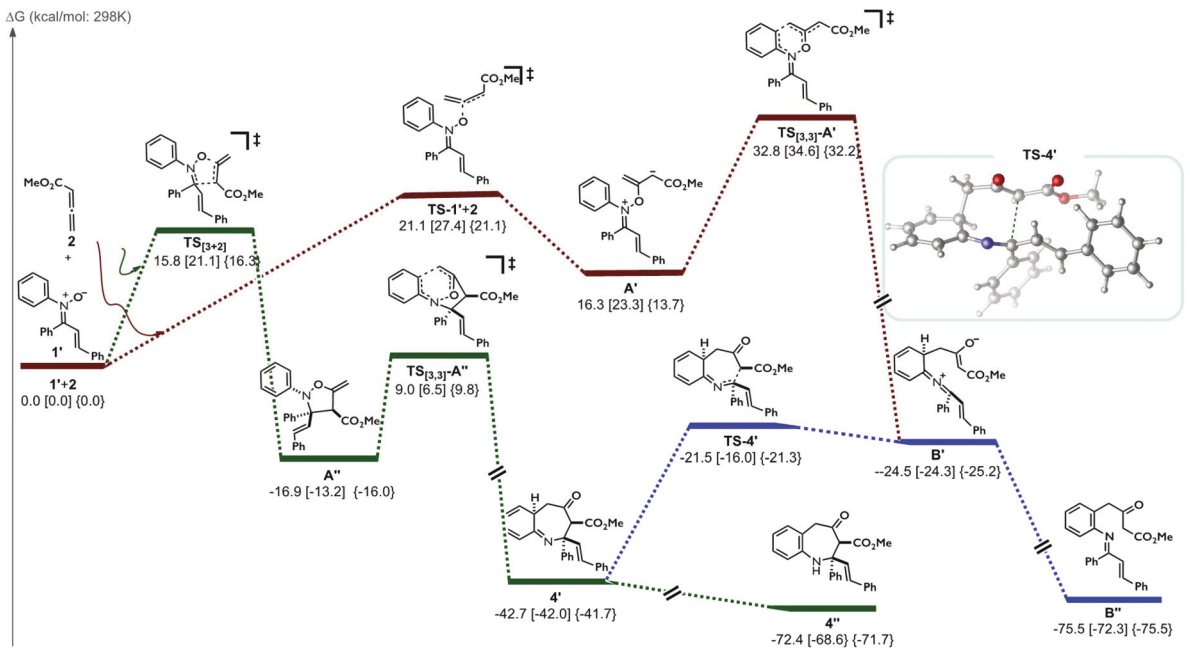

Fig. 1 Reaction profile. Free energies (kcal mol^{-1}) were computed using M06-2X/6-31G(d,p)-CPCM(chloroform, DLPNO-CCSD(T)/def2-TZVPP-CPCM(chloroform)//M06-2X/6-31G(d,p)-CPCM(chloroform) [in brackets] and M06-2X/6-31G(d,p)-CPCM(water)//M06-2X/6-31G(d,p)-CPCM (chloroform).

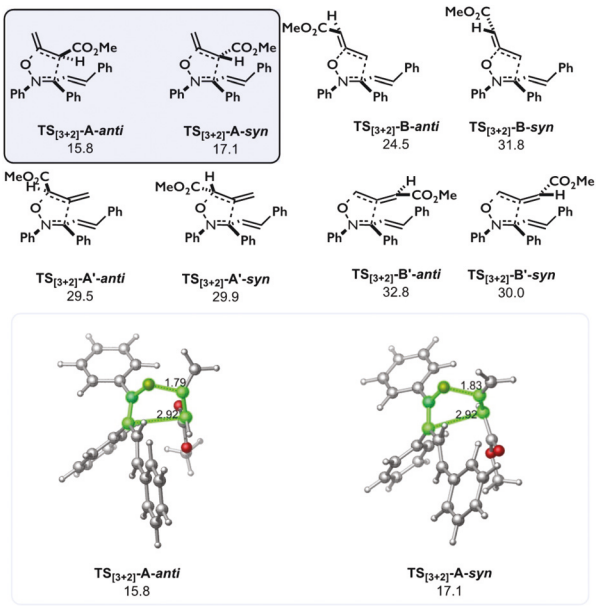

Scheme 3 Relative barriers for [3 + 2] cycloaddition step between nitrone and allenoate. Free energies (kcal mol^{-1}) were computed using M06-2X/6-31G(d,p)-CPCM(chloroform).

look at the lowest energy transition states (Scheme 3, inset) reveals a very asynchronous transition state, in which the most nucleophilic oxygen of the nitrone forms the bond with most electrophilic carbon of allene before undergoing C–C bond formation. Thus, these asynchronous transition state structures can be viewed (and used to rationalize the chemo- and regioselectivity) as formation of the incipient more stable enolate-like structure (along the concerted pathway) that will then undergo nucleophilic attack to form the C–C bond. Overall, the first step in the reaction between aryl nitrones and allenes is a highly chemo- and regio-selective [3 + 2] cycloaddition leading to the formation of anti and syn **A″** diastereomers (Fig. 1, green). Only the lowest energy isomer is shown for simplicity.

From cycloaddition adduct **A″**, we located a subsequent [3,3]-sigmatropic dearomatization step (*via* **TS$_{[3,3]}$-A″**) that leads directly to a highly exergonic (*ca.* −42 kcal mol^{-1}) seven-member ring **4′**, which is a precursor to benzazepine **4″**. Overall, the barrier for this step is 19–26 kcal mol^{-1} which is feasible at the experimental conditions. Further, given that the barrier to undergo the [3 + 2] cycloaddition is facile and that the subsequent dearomatization step is significantly higher in energy, we predict that through careful control of the temperature it may be possible to observe (and even isolate) of cycloaddition adducts (*i.e.*, **A″**).[10] Alternatively, if **A″** is synthesized by an alternative (independent) method, subjecting this species to thermal reaction is expected to yield similar products as the reaction of **1″** + **2**.

Importantly, calculations show that imine **4′** can lead to both experimentally observed products **4″** and **B″**. Specifically, the barrier to undergo a retro-Mannich reaction (*via* **TS-4′**) from **4′** is 20–26 kcal mol^{-1} leading to highly exergonic **B″** (Fig. 1, blue). Further, consistent with previous experimental results, the formation of **4″**, presumably *via* rearomatization of **4′** (not calculated), is irreversible (barrier to equilibrate to **B″** *via* **TS-4′** is >50 kcal mol^{-1}!). Overall, the [3 + 2], dearomative [3,3]-sigmatropic rearrangement, retro-Mannich cascade reaction (green-blue) is energetically favored than the addition to allene, [3,3], and H-transfer cascade reaction (red) leading to the formation of both **4″** and **B″** (Fig. 1). Notably, **4′** is the bifurcating point in this cascade reaction in which an H-shift (not calculated) will form the more energetically stable benzazepine **4″** while a retro-Mannich reaction (via **TS-4′**) will lead to the azallenium intermediate **B′**, which can then isomerize (not calculated) to the more thermodynamically stable imine **B″**.[21]

Further, a closer look at the retro-Mannich transition state **TS-4′** reveals a very late and asynchronous transition state (Fig. 1, inset). This implies that, consistent with Hammond's postulate, the transition state resembles the highly endergonic azallenium intermediate **B′** which is expected to have a significant build-up of positive charge at nitrogen. As such, we expect that through careful tuning of the electronics of the group *meta* to the azallenium moiety one can raise or lower the barrier for the retro-Mannich step (*e.g.*, **TS-4′**). Indeed, quantum mechanical calculations show that energy difference between *meta*-substituted **4′** and **B″** intermediates (and hence

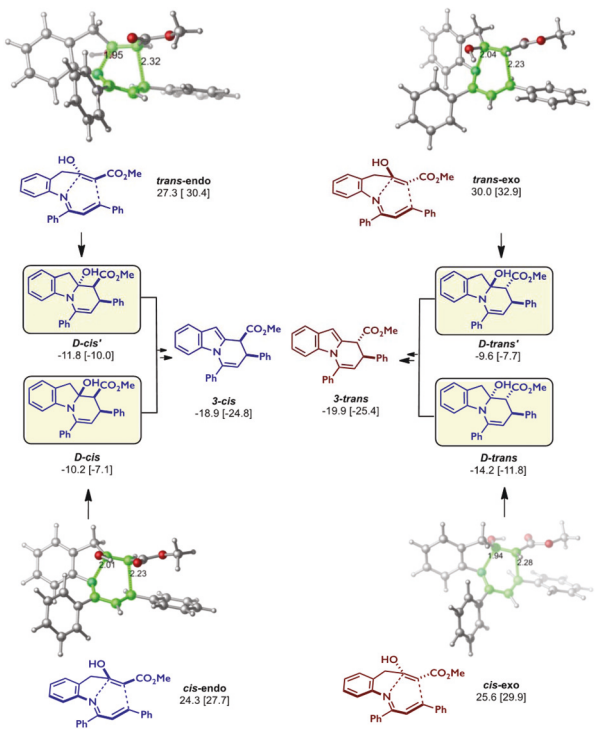

Scheme 4 Relative barriers for [4 + 2] cycloaddition. Free energies (kcal mol^{-1}; with respect to **B″**) were computed using M06-2X/6-31G(d,p)-CPCM(chloroform)//B3LYP/6-31G(d,p)-CPCM(chloroform) and DLPNO-CCSD(T)/def2-TZVPP-CPCM(chloroform)//B3LYP/6-31G(d,p)-CPCM(chloroform) [in brackets].

the barrier) decreases with electron-donating groups (*e.g.*; H = 18.2 *vs.* *m*-OMe = 16.7 kcal mol^{-1}) and increases with more electron-withdrawing groups (*m*-Cl = 18.7 and *m*-CF_3 = 20.2 kcal mol^{-1}). Thus, these results predict that one might be able to diverge the selectivity to **B″** with strongly electron-donating groups at the meta position of the aryl ring in the aryl-nitrone or hinder the formation of this intermediate with strongly electron-withdrawing aryl nitrones.

Having established the feasibility and bifurcating pathways leading to adducts **4″** and **B″** from dearomatized dihydrobenzoazepinone **4′**, we then explored the thermal barriers for the [4 + 2] cycloaddition from the corresponding enol isomer of **B″**.[11] Previously, Anderson showed that at room temperature the cascade reaction could be stopped at the enanimo-enol **C** intermediate (Scheme 2).[11] Specifically, control experiments by Anderson demonstrated the formation of both imine **B** and benzazepine **4** in the thermal reaction (at 25 °C) between nitrone and allenes (Scheme 2).[11] When the reaction mixture of **B** and **4** was heated to 80 °C, the reaction produce the dihydropyrido[1,2-*a*]indole **3**, presumably from the hetero Diels–Alder reaction/dehydration sequence (Scheme 2).[11] Taken together, these results imply that formation of **B** and **4** is feasible at lower temperatures but the formation of **3** (from **B**) requires elevated temperatures in order to overcome the presume higher overall barrier (*vide infra*) to undergo the [4 + 2] cycloaddition.

Indeed, as shown in Scheme 4, the overall barriers for the thermal [4 + 2] cycloaddition are high (>24–33 kcal mol^{-1} depending on the method) thus explaining the need for higher temperatures to form **3**. Further, the [4 + 2] cyclization is exothermic (8–14 kcal mol^{-1}) leading to the corresponding diastereomeric fused indoles (**D-*cis***, **D-*cis*′**, **D-*trans***, and **D-*trans*′**) which can then undergo facile dehydration to form the much more thermodynamically (downhill by 20–26 kcal mol^{-1}) stable and nearly isoenergetic dihydropyrido[1,2-*a*]indoles **3-*cis*** and **3-*trans***. A closer look at the [4 + 2] transition state structures (Scheme 4) reveals that the lowest energy cycloaddition transition state structures (***cis-endo*** and ***cis-exo***) benefit from an intramolecular hydrogen bond between the OH and CO_2Me of the enol moiety (Scheme 4, bottom). Moreover, the lowest energy [4 + 2] transition state structure (*i.e.*, ***cis-endo***) will lead to the formation of the *cis* dihydroindole, after dehydration (not calculated), while the lowest energy transition state leading to the *trans* dihydroindole (*i.e.*, ***cis-exo***) state is only *ca.* 1 kcal mol^{-1} higher in energy. The small energy difference implies that subtle changes to the reaction condition could tilt the selectivity as was shown experimentally. Specifically, the selectivity for the uncatalyzed [4 + 2]

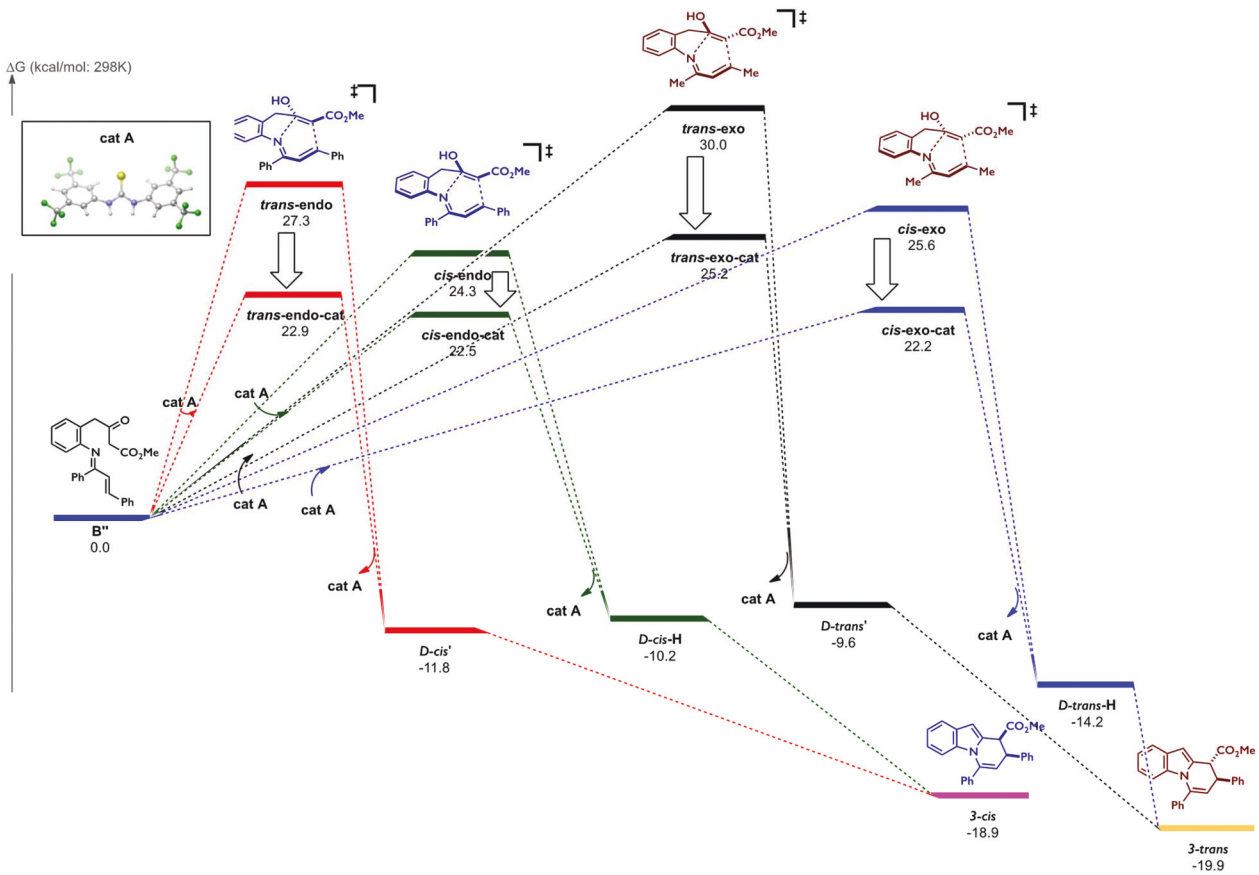

Fig. 2 Reaction profile for thermal and thiourea-catalyzed [4 + 2] cycloaddition. Free energies (kcal mol^{-1}) were computed using M06-2X/6-31G(d,p)-CPCM(chloroform)//B3LYP/6-31G(d,p)-CPCM(chloroform).

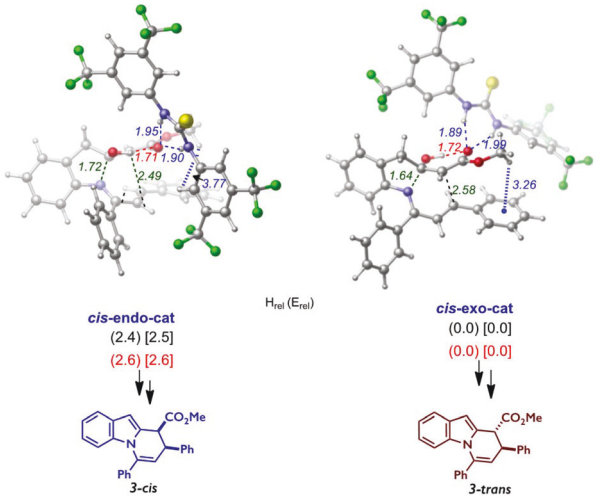

Scheme 5 Relative enthalpies (in parenthesis) and electronic energies (in brackets) are in kcal mol^{-1} computed using M06-2X/6-31G(d,p)-CPCM(chloroform)//B3LYP/6-31G(d,p)-CPCM(chloroform) and (red) M06-2X/6-31G(d,p)-CPCM(water)//B3LYP/6-31G(d,p)-CPCM(chloroform).

product (at elevated temperatures, Scheme 1) was shown to depend on the solvent and additives and varies from *trans* being favoured (3.5: 1 *trans*/*cis*) to *cis* as major product (1: 1.6 *trans*/*cis*). Finally, the diastereomeric transition states with the *trans* relationship between the OH and CO_2Me (***trans-endo*** and ***trans-exo***) are higher in energy (3–6 kcal mol^{-1}), presumably due to the lack of intramolecular H-bond. In all cases, the *endo* transition state structures that benefit from secondary orbital interactions,[22] are lower in energy. Also, the ***cis-endo*** and ***trans-exo*** transition states are further destabilized due to 1,3-strain between the C–OH and the C–Me bonds. Overall, these interactions play a crucial role in the low diastereoselectivity of the thermal hetero-Diels–Alder reaction.

Previously, it was shown that thioureas can increase the selectivity of the Diels–Alder products from *ca.* 1 : 1 up to 15 : 1 *trans* : *cis* and shown to promote the formation of final product from imine **B** (presumably by accelerating the Diels–Alder/dehydration step; Fig. 2). To gain insights at the effect of thiourea in controlling reactivity and selectivity, we performed computational modelling using the full system and thiourea catalyst used in experiment with focus on the Diels–Alder step.[23] As shown in Fig. 2, the thiourea **A** catalyst lowers the barriers of all the diastereomeric Diels–Alder transition states by 2–5 kcal mol^{-1}. Thus, in agreement with experiment, the [4 + 2] cycloaddition step is expected to be accelerated by the addition of thiourea catalyst. Given the errors associated with free energies,[24] we analysed in detail the relative energies and enthalpies (that are less prone to errors) to get a better representation of the relative energies between the lowest transition states leading to **3-*cis*** and **3-*trans*** (Scheme 5). As shown in Scheme 5, closer inspection at the lowest energy diastereomeric transition states ***cis-endo*-cat** and ***cis-exo*-cat** reveals a *ca.* 2 kcal mol^{-1} energetic preference, in both chloroform and highly polar solvent, for ***cis-exo*-cat**. This energetic preference predicts, in agreement with experiment, the formation of **3-*trans*** as the major diastereomer. Notably, both diastereomeric transition states are highly asynchronous (C–N bond forms first) and both benefit from an intramolecular hydrogen bond. However, the much more asynchronous ***cis-exo*-cat** transition state presumably benefits from a stronger C–H···π interaction between the ester moiety and aryl ring of the substrate as evident from the much shorter C–H distance (3.26 *vs.* 3.77 Å).

Conclusions

Cascade reactions between nitrones and allenes have been shown to be sensitive to reaction conditions and often require elevated temperatures. In this work, we used quantum mechanical calculations to investigate the mechanism of these transformations. Overall, high-level quantum mechanical calculations favor the cascade reaction initiated by a highly chemo- and regioselective [3 + 2] dipolar cyclization. Furthermore, calculations revealed a fused, dearomatized imine heterocycle as a branching point leading to two experimentally observed intermediates. Finally, calculations on the hetero Diels–Alder step are consistent with the barrier lowering with the H-bond catalysts and identify a C–H···π interaction as critical element for controlling diastereoselectivity. We hope that this work will guide future reaction design to control divergent pathways in these cascade reactions.

Conflicts of interest

There are no conflicts to declare.

Acknowledgements

The authors are grateful for the financial support provided by the NSF (CAREER, 1751568 to O.G.) and the University of Maryland College Park for start-up funds. We are thankful for the computational resources from UMD Deepthought2 and MARCC/BlueCrab HPC clusters and XSEDE (CHE160082 and CHE160053).

Notes and references

1 (*a*) C. Serba and N. Winnssinger, *Eur. J. Org. Chem.*, 2013, 4195–4214; (*b*) K. C. Nicolaou, D. J. Edmonds and P. G. Bulger, *Angew. Chem., Int. Ed.*, 2006, **45**, 7134–7186.

2 (*a*) M. D. Delost, D. T. Smith, B. J. Anderson and J. T. Njardarson, *J. Med. Chem.*, 2018, **61**, DOI: 10.1021/acs.jmedchem.8b00876; (*b*) K. A. Scott and J. T. Njardarson, *Top. Curr. Chem.*, 2018, **376**, 1–34; (*c*) N. A. McGrath, M. Brichacek and J. T. Njardarson, *J. Chem. Educ.*, 2010, **87**, 1348–1349.

3 C. Cabrelle and O. Reiser, *J. Org. Chem.*, 2016, **81**, 10109–10125.
4 J. J. Tufariello, S. A. Ali and O. H. Klingele, *J. Org. Chem.*, 1979, **44**, 4213–4215.
5 (*a*) M. C. Aversa, G. Cum and N. Uccella, *J. Chem. Soc. D*, 1971, 156–157; (*b*) G. Cum, G. Sindona and N. Uccella, *J. Chem. Soc., Perkin Trans. 1*, 1976, 719–721.
6 (*a*) S. Blechert, *Liebigs Ann. Chem.*, 1985, **1985**, 673–682; (*b*) J. Wilkens, A. Kühling and S. Blechert, *Tetrahedron*, 1987, **43**, 3237–3246.
7 (*a*) A. Padwa, M. Matzinger, Y. Tomioka and M. K. Venkatramanan, *J. Org. Chem.*, 1988, **53**, 955–963; (*b*) A. Padwa, W. H. Bullock, D. N. Kline and J. Perumattan, *J. Org. Chem.*, 1989, **54**, 2862–2869.
8 (*a*) M. P. S. Ishar and K. Kumar, *Tetrahedron*, 1999, **40**, 175–176; (*b*) A. Kapur, K. Kumar, L. Singh, P. Singh, M. Elango, V. Subramanian, V. Gupta, P. Kanwal and M. P. S. Ishar, *Tetrahedron*, 2009, **65**, 4593–4603; (*c*) S. S. Bhella, A. P. S. Pannu, M. Elango, A. Kapoor, M. Hundal and M. P. S. Ishar, *Tetrahedron*, 2009, **65**, 5928–5935.
9 W. H. Pecak, J. Son, A. J. Burnstine and L. L. Anderson, *Org. Lett.*, 2014, **16**, 3440–3443.
10 L. L. Anderson, M. A. Kroc, T. W. Reidl and J. Son, *J. Org. Chem.*, 2016, **81**, 9521–9529.
11 (*a*) D.-L. Mo, D. J. Wink and L. L. Anderson, *Chem. – Eur. J.*, 2014, **20**, 13217–13225; (*b*) M. A. Kroc, A. Prajapati, D. J. Wink and L. L. Anderson, *J. Org. Chem.*, 2018, **83**, 1085–1094.
12 For the catalytic asymmetric synthesis using chiral squaramide catalysts, see: W. H. Pace, D.-L. Mo, T. W. Reidl, D. J. Wink and L. L. Anderson, *Angew. Chem., Int. Ed.*, 2016, **55**, 9183.
13 Y. Zhao and D. Truhlar, *Theor. Chem. Acc.*, 2008, **120**, 215–241.
14 Y. Takano and K. N. Houk, *J. Chem. Theory Comput.*, 2005, **1**, 70–77.
15 M. J. Frisch, *GAUSSIAN09, Revision E*, Gaussian Inc., Wallingford, CT, 2009.
16 (*a*) F. Neese, *Wiley Interdiscip. Rev.: Comput. Mol. Sci.*, 2012, **2**, 73–78; (*b*) C. Riplinger, B. Sandhoefer, A. Hansen and F. Neese, *J. Chem. Phys.*, 2013, **139**, 134101–134113.
17 (*a*) D. G. Liakos, M. Sparta, M. K. Kesharwani, J. M. L. Martin and F. Neese, *J. Chem. Theory Comput.*, 2015, **11**, 1525–1539; (*b*) E. Paulechka and A. Kazakov, *J. Phys. Chem. A*, 2017, **121**, 4379–4387.
18 For a recent examples, see: J. P. Phelan, S. B. Lang, J. S. Compton, C. B. Kelly, R. Dykstra, O. Gutierrez and G. A. Molander, *J. Am. Chem. Soc.*, 2018, **140**, 8037–8047.
19 K. Kumar, S. M. Woo, T. Siu, W. A. Cortopassi, F. Duarte and R. S. Paton, *Chem. Sci.*, 2018, **9**, 2655–2665.
20 C. Y. Legault, *1.0b*, Université de Sherbrooke, Sherbrooke, Canada, 2009, http: //www.cylview.org.
21 (*a*) H. Frey, A. Mehlhorn and K. Ruehlmann, *Tetrahedron*, 1987, **43**, 2945–2954; (*b*) M. Al-Talib, I. Jibril, J. C. Jochims and G. Huttner, *Tetrahedron*, 1985, **41**, 527–536; (*c*) M. Al-Talib and J. C. Jochims, *Chem. Ber.*, 1984, **117**, 3222–3230.
22 K. N. Houk and R. W. Strozier, *J. Am. Chem. Soc.*, 1973, **95**, 4094–4096.
23 To address reviewers concerns in due time, we have explore this step using B3LYP/6-31G(d,p)-CPCM(choloroform) optimizations since other methods were proving challenging to converge and performed subsequent single point energies using M06-2X/6-31G(d,p)-CPCM in both chloroform and water, DLPNO-CCSD(T)/def2-TZVPP-CPCM(chloroform), and B3LYP-D3/6-31G(d,p)-CPCM(chloroform).
24 P. H.-Y. Cheong, C. Y. Legault, J. M. Um, N. Celebi-Olcum and K. N. Houk, *Chem. Rev.*, 2011, **111**, 5042–5137.

